Anisotropic Upper Critical Field of $LuNi_2B_2C$

V. Metlushko, U. Welp, A. Koshelev, I. Aranson, and G. W. Crabtree
Materials Science Division, Argonne National Laboratory, Argonne, Illinois 60439

P. C. Canfield
Ames Laboratory and Department of Physics and Astronomy, Iowa State University, Ames, Iowa 50011
(Received 15 April 1997)

The upper critical field, H_{c2}, of $LuNi_2B_2C$ has been determined from the temperature dependence of the magnetization. A temperature dependent anisotropy within the basal plane which decreases from a value of 1.1 at 4.5 K to a value of 1.0 at T_c and an almost temperature independent out-of-plane anisotropy have been observed. Near T_c the upper critical field along all directions shows a strong upward curvature. These features of H_{c2} can be explained quantitatively using a nonlocal extension of the Ginzburg-Landau equations. The Fermi velocity averages determined from these measurements and those obtained in band structure calculations are in good agreement. [S0031-9007(97)03913-6]

PACS numbers: 74.60.Ec

Recently, a new family of rare earth (Re) based superconductors with the composition $ReNi_2B_2C$ has been discovered, where Re = Lu, Y, Tm, Er, Ho, and Dy [1]. All members of this family have a body-centered tetragonal crystal structure composed of alternating layers of Ni_2B_2 and ReC [2]. The values of T_c range from about 16 K in $LuNi_2B_2C$ to 6 K in $DyNi_2B_2C$ and roughly scale with the de Gennes factor across the series [3,4]. The magnetic variants, Re = Er, Ho, Tm, undergo a transition to antiferromagnetic order within the superconducting state [3,5,6] whereas in $DyNi_2B_2C$ the superconducting transition occurs within the antiferromagnetic state [4]. The availability of large, high-quality single crystals [6] allows the study of the interplay of the superconducting and magnetic ground states and their anisotropies. In particular, the interaction of superconductivity and magnetism was proposed as the origin of a vortex lattices (VL) with square symmetry for magnetic fields along the tetragonal axis observed in $ErNi_2B_2C$ using small angle neutron scattering (SANS) [7]. The observation of similar square lattices in nonmagnetic $LuNi_2B_2C$ using scanning tunneling microscopy (STM) [8] and SANS [9] indicates a different origin in this material. In recent theoretical work based on the London model [10] and on the Ginzburg-Landau (GL) model [11] it was shown that anisotropic energy contributions arising from nonlocal corrections of sufficient strength can stabilize a square vortex lattice. Within GL theory the anisotropy of H_{c2} in the basal plane can be correlated with the occurrence of a square VL, with the square lattice being stable for anisotropies $H_{c2}^{\langle 100\rangle}/H_{c2}^{\langle 110\rangle}$ larger than approximately 1.03.

Here, we present measurements of the upper critical field as determined from the temperature dependence of the magnetization. Along all orientations, H_{c2} has an upward curvature near T_c. We observe a temperature dependent anisotropy within the basal plane decreases from a value of $H_{c2}^{\langle 100\rangle}/H_{c2}^{\langle 110\rangle} = 1.1$ at 4.5 K to 1.0 at T_c. The average out-of-plane anisotropy $0.5(H_{c2}^{\langle 100\rangle} + H_{c2}^{\langle 110\rangle})/H_{c2}^{\langle 001\rangle}$ is essentially temperature independent with a value of 1.16. The angular dependence of H_{c2} within the basal plane as well as the curvature of H_{c2} can be described quantitatively with a nonlocal extension [12] of Gorkov's derivation [13] of the GL equations. Fermi velocity averages determined from the measurements presented here are in good agreement with those obtained from recent band structure calculations [14,15]. These unusual features of the upper critical field as well as the occurrence of a square vortex lattice arise from two materials properties: the anisotropic Fermi surface and the high purity of the samples which allows microscopic Fermi surface anisotropy to manifest itself in macroscopic phenomena through nonlocal effects.

The sample studied here has a mass of 2.95 mg and $T_c = 15.8$ K. It was grown using Ni_2B [6] flux and is a piece of the crystal that was used in STM studies of the square VL [8]. Figure 1(a) shows the temperature dependence of the magnetization in various fields applied parallel to $\langle 100\rangle$. Data for $\langle 010\rangle$ and $\langle 001\rangle$ are qualitatively similar. In contrast to high-temperature superconductors in which fluctuation effects cause a substantial broadening of the transition with increasing field, the transition curves for $LuNi_2B_2C$ shift to lower temperatures in an almost parallel fashion. H_{c2} is determined using the linear extrapolations indicated in the figure. Figure 1(b) shows the temperature dependence of the magnetization in a field of 3 T applied along $\langle 100\rangle$, $\langle 110\rangle$, and $\langle 001\rangle$, respectively. An anisotropy among all three orientations is clearly seen. The results are summarized in the phase diagram in Fig. 2. H_{c2} for the three orientations has an upward curvature near T_c which below about 10 K crosses over into a linear temperature dependence. These results are consistent with similar findings on single crystal YNi_2B_2C [16] and polycrystalline YNi_2B_2C [17] and $LuNi_2B_2C$ [18]. The in-plane anisotropy $H_{c2}^{\langle 100\rangle}/H_{c2}^{\langle 110\rangle}$ and the average out-of-plane anisotropy $0.5(H_{c2}^{\langle 100\rangle} + H_{c2}^{\langle 110\rangle})/H_{c2}^{\langle 001\rangle}$

 0031-9007/97/79(9)/1738(4)$10.00

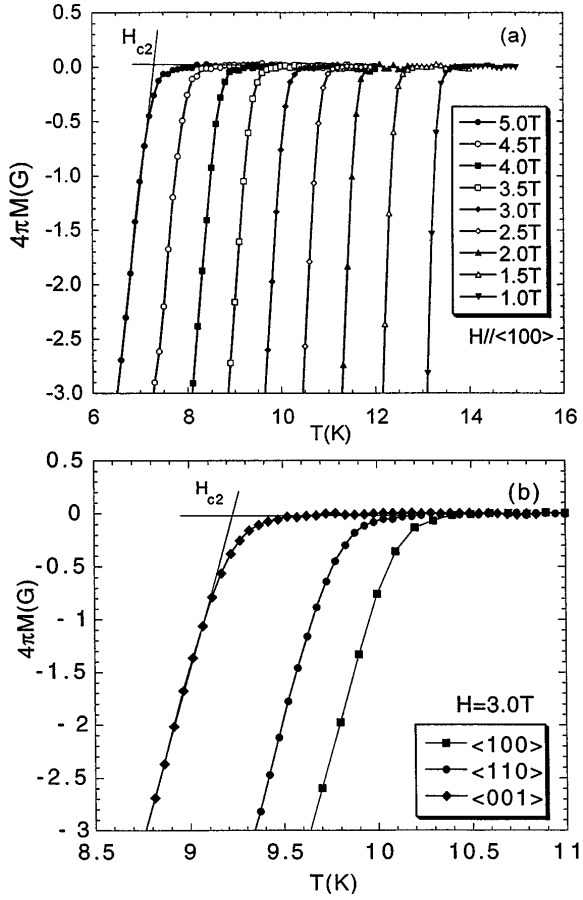

FIG. 1. (a) Temperature dependence of the magnetization in several fields applied parallel to the ⟨100⟩ direction. The upper critical field is determined through linear extrapolations as indicated in the figure. (b) Temperature dependence of the magnetization in a field of 3 T applied along the crystallographic ⟨100⟩, ⟨110⟩, and ⟨001⟩ directions.

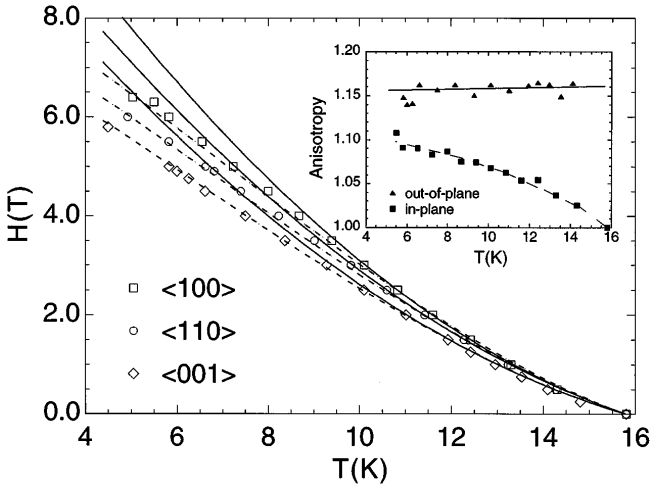

FIG. 2. Temperature dependence of the upper critical field along the three crystallographic directions. The solid lines are fits according to Eqs. (1) and (2) as described in the text and the dotted lines are fits including a $(1 - T/T_c)^3$ term. The inset shows the temperature dependence of the in-plane and the average out-of-plane anisotropies. The dashed line is a guide to the eye; the solid line is a fit to Eqs. (1) and (2).

are shown in the inset. The out-of-plane anisotropy is essentially temperature independent at a value of 1.16, whereas the in-plane anisotropy decreases from about 1.1 to 1.0 on approaching T_c. The value $H_{c2}^{\langle 100\rangle}/H_{c2}^{\langle 110\rangle} \approx 1.03$ is reached around 14 K, indicating that below this temperature a VL with square symmetry can exist [8,11]. Anisotropy due to nonlocal effects disappears while approaching T_c, whereas anisotropy caused by anisotropic effective masses is temperature independent in standard GL theory. Therefore, the out-of-plane anisotropy of 1.16 while approaching T_c corresponds to an effective mass anisotropy of $m_{\langle 001\rangle}/m_{\langle 100\rangle} = 1.34$, which is in good agreement with the value 1.35 predicted from band structure calculations [14,15]. In spite of the layered structure the electronic anisotropy of $LuNi_2B_2C$ is rather weak. It is, however, significantly larger than the value of 1.01 observed in YNi_2B_2C [19].

Local GL theory including effective mass anisotropy does not account for the occurrence of anisotropy in the tetragonal basal plane nor for the positive curvature of $H_{c2}(T)$. These results are reminiscent of anisotropic effects previously observed in cubic materials such as clean Nb, V [20] and V_3Si [21] or in the basal plane of uniaxial materials such as $Cs_{0.1}WO_{2.9}F_{0.1}$ [22]. These effects arise from nonlocal effects [12,23] which in sufficiently clean materials become observable when the transport mean free path becomes larger than the superconducting coherence length. Within microscopic theory nonlocal corrections have been incorporated into Gorkov's derivation of the GL equations through terms of the form $\langle|(\mathbf{v}\Pi)^n\psi|^2\rangle$ $(n \geq 2)$ for cubic [12,23] as well as for uniaxial systems [24]. Here, $\mathbf{v}$ is the Fermi velocity, $\Pi = \nabla - 2\pi i/\Phi_0\mathbf{A}$ is the gauge invariant derivative, ψ is the superconducting order parameter, and $\langle\cdots\rangle$ represents the average over the Fermi surface. The anisotropy arising from these corrections is determined by the anisotropy of the Fermi surface and/or of the superconducting pairing interaction. For the case of isotropic pairing interactions and for the clean limit H_{c2} within the tetragonal basal plane is given by

$$H_{c2}^a(T,\phi) = h_{c2}^a t\left[1 + \left(-\frac{3}{2} + 0.3406C\right)t + 0.3406At\cos(4\phi)\right], \quad (1)$$

with $t = 1 - T/T_c$. ϕ is measured with respect to the ⟨100⟩ direction. This relation contains nonlocal corrections in lowest order $(n = 2)$ and the temperature dependence up to second order in t. A similar relation has recently been applied for the study of the upper critical field of $La_{2x}Sr_xCuO_4$ [25]. Here, $-h_{c2}^a/T_c$ is the initial slope of the upper critical field. C and A contain averages of the Fermi velocity; $C = (2\langle\nu_x^2\nu_z^2\rangle + \langle\nu_z^4\rangle)/\langle\nu_z^2\rangle^2 + 0.75(\langle\nu_x^4\rangle + \langle\nu_x^2\nu_z^2\rangle)/\langle\nu_x^2\rangle^2$

and $A = (\langle v_x^4 \rangle - 3\langle v_x^2 v_y^2 \rangle)/4\langle v_x^2 \rangle^2$. The term containing C contributes an isotropic upward curvature to H_{c2}, whereas the term with A provides an anisotropic upward curvature. For a spherical Fermi surface, $C = 4.8$ and $A = 0.0$. Within a phenomenological approach it was shown [8] that the in-plane anisotropy of H_{c2} is related to the stability of the square vortex lattice.

The expression corresponding to Eq. (1) for H_{c2} along $\langle 001 \rangle$ is given by

$$H_{c2}^c(T) = h_{c2}^c t\left[1 + \left(-\frac{3}{2} + 0.3406D\right)t\right], \quad (2)$$

with $D = 2(\langle v_x^4 \rangle + \langle v_x^2 v_y^2 \rangle)/\langle v_x^2 \rangle^2$.

In the following the parameters h_{c2^a}, h_{c2^c}, A, C, and D appearing in Eqs. (1) and (2) are determined from fits to the data. Equations (1) and (2) represent expansions valid near T_c whose exact range of applicability is not known *a priori.* In addition, a direct fit to Eq. (1) requires the simultaneous determination of three coefficients. Therefore, it is more convenient to first find A and C by evaluating the relative basal plane anisotropy $\Gamma = (H_{c2}^{\langle 100 \rangle} - H_{c2}^{\langle 110 \rangle})/(H_{c2}^{\langle 100 \rangle} + H_{c2}^{\langle 110 \rangle}) = 0.3406At/[1 + (-1.5 + 0.3406C)t]$ as shown in Fig. 3. A least-squares fit, indicated by the solid line, describes the data well over the entire temperature range. The values for C and A are $C = 9.4$ and $A = 0.43$, respectively, which change to 9.1 and 0.42 when restricting the fitted temperature range to $t < 0.35$. From band structure calculations [14,15] the corresponding values are $C = 8.1$ and $A = 0.63$, in reasonable agreement with our upper critical field analysis.

The reduced anisotropy as compared to the band structure prediction can be accounted for by the impurity scattering that is present in the sample. Using the Drude formula as a transport mean free path $l \approx 320$ Å can be estimated from the residual resistivity of 1.7 $\mu\Omega$ cm measured on a third piece of the original crystal [26], and from the band structure value for the Fermi velocity $v = \langle v^2 \rangle^{1/2} = 2.3\ 10^7$ cm/sec and the density of states of 4.8 states/(eV primitive cell) [14,15]. The superconducting coherence length ξ_0 can be estimated using $\xi_0 = hv/\pi\Delta$, giving $\xi_0 = 200$ Å with $\Delta = 2.2$ meV [8]. Alternatively, ξ_0 can be deduced from the initial slope of the upper critical field which is not affected by nonlocal effects: $\xi_0 = 0.54[-\Phi_0/T_c(dH_{c2}/dT)]^{1/2} \approx 130$ Å. Thus, an impurity parameter of $\alpha = 0.88\xi_0/l \approx 0.5$ identifies our $LuNi_2B_2C$ samples as approaching the clean limit.

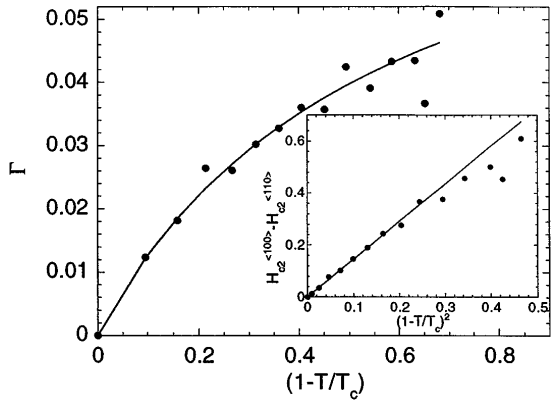

FIG. 3. Temperature dependence of $\Gamma = (H_{c2}^{\langle 100 \rangle} - H_{c2}^{\langle 110 \rangle})/(H_{c2}^{\langle 100 \rangle} + H_{c2}^{\langle 110 \rangle})$. The solid line is a least-squares fit according to Eq. (1). The inset shows $H_{c2}^{\langle 100 \rangle} - H_{c2}^{\langle 110 \rangle}$ as a function of $(1 - T/T_c)^2$.

h_{c2^a} is determined from fitting the experimental data above 9 K to the expression $H_{c2}^{\langle 100 \rangle} - H_{c2}^{\langle 110 \rangle} = 0.6812h_{c2}^a At^2$ as shown in the inset of Fig. 3, yielding $h_{c2^a} = 5.1$ T. Deviations from the simple quadratic temperature dependence below 9 K are related to the fact that Eqs. (1) and (2) do not capture the downward curvature of H_{c2} which is observed at low temperatures. The average out-of-plane anisotropy can be fitted with Eqs. (1) and (2) (see inset of Fig. 2) yielding $D = 9.5$. The value from band structure calculations is $D = 9.3$. Since D and C are almost identical the out-of-plane anisotropy is essentially temperature independent with $h_{c2}^a/h_{c2}^c = 1.16$ representing the conventional effective mass anisotropy. The temperature dependences of H_{c2} predicted by Eqs. (1) and (2) using the parameters determined above are shown as solid lines in Fig. 2. The absolute values, the curvature and anisotropy of the experimental data at temperatures above 10 K is well described, whereas at lower temperatures the absolute values of H_{c2} are significantly overestimated as discussed above. The fit of the low-temperature data of H_{c2} can be significantly improved by incorporating a term Et^2 in the square brackets in Eqs. (1) and (2) as shown by the dotted lines in Fig. 2. This term arises from the next order in the GL expansion (see Ref. [23]) as well as from nonlocal effects. The explicit expression for E contains isotropic (in the basal plane) and $\cos(4\phi)$ and $\cos(8\phi)$ dependent contributions as well as Fermi surface averages of second, fourth, and sixth order [24] where the sixth order averages have not yet been determined from band structure calculations. The numerical values of E determined from the fits in Fig. 2 are -1.2 for $\langle 100 \rangle$, -0.95 for $\langle 110 \rangle$, and -1.1 for $\langle 001 \rangle$. In this fitting procedure the values of $A = 0.5$, $C = 9.7$, and $D = 10.2$ are essentially the same as those determined from the high-temperature regime.

The importance of terms arising from higher order nonlocal corrections to the basal plane anisotropy can be inferred independently from the presence of contributions proportional to $\cos(8\phi)$ in the angular dependence of H_{c2} as shown in Fig. 4 at 6 and 10 K. The dashed lines are the predictions according to Eq. (1) with values for h_{c2^a}, C, and A as determined in Fig. 3. The angular dependence can be reproduced well, however, there are systematic deviations. Slightly improved fits including a term $m_4 \cos(8\phi)$ in the square brackets of Eq. (1)

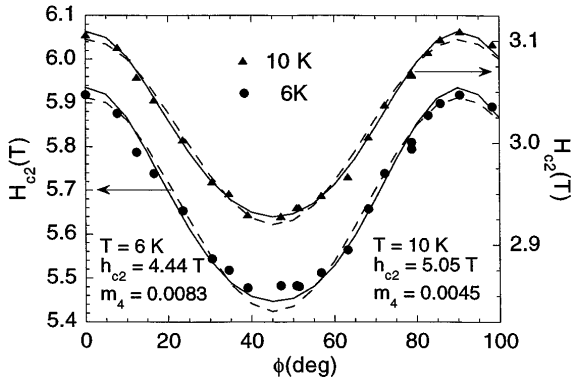

FIG. 4. Angular dependence of the upper critical field within the tetragonal basal plane at 6 and at 10 K. The dashed lines are fits according to the expression in the text, the solid lines are fits including a term proportional to $\cos(8\phi)$.

are shown as solid lines with fit coefficients given in the figure. It is found that the amplitude of the $\cos(8\phi)$ term, m_4, is one order of magnitude smaller than that of the $\cos(4\phi)$ term, $0.3406tA$, indicating that in the temperature range studied here higher order terms are relatively unimportant in the analysis of the in-plane anisotropy of H_{c2}.

In conclusion, the determination of the upper critical field of $LuNi_2B_2C$ from the temperature dependence of the magnetization reveals a pronounced, temperature dependent anisotropy within the tetragonal basal plane reaching 1.1 at 4.5 K and an almost temperature independent out-of-plane anisotropy of 1.16. Near T_c the upper critical field along all directions shows a strong upward curvature. These features of H_{c2} can be explained quantitatively using nonlocal extensions of the GL equations. The Fermi velocity averages determined from these measurements and those obtained in band structure calculations are in good agreement. In $LuNi_2B_2C$ nonlocal effects arising from the anisotropic Fermi surface and low electronic scattering lead to the observed features of the upper critical field and to a square (rather than hexagonal) vortex lattice.

This work was supported by the U.S. Department of Energy under Contract No. W-31-109-ENG-38 (V. M., U. W., G. W. C., A. E. K., I. A.) and under Contract No. W-740-ENG-82 (P. C. C.). We would like to thank Vladimir Kogan for many stimulating discussions and Peter Gammel for communicating his results prior to publication.

[1] R. J. Cava *et al.,* Nature (London) **367**, 252 (1994); R. Nagarajan *et al.,* Phys. Rev. Lett. **72**, 274 (1994).
[2] T. Sigrist *et al.,* Nature (London) **367**, 254 (1994).
[3] H. Eisaki *et al.,* Phys. Rev. B **50**, 647 (1994).
[4] B. K. Cho, P. C. Canfield, and D. C. Johnston, Phys. Rev. B **52**, 3844 (1995).
[5] C. Godart *et al.,* Phys. Rev. B **51**, 489 (1995); A. I. Goldman *et al.,* Phys. Rev. B **50**, 9668 (1994); B. K. Cho *et al.,* Phys. Rev. B **52**, 3676 (1995).
[6] B. K. Cho *et al.,* Phys. Rev. B **52**, 3684 (1995).
[7] U. Yaron *et al.,* Nature (London) **382**, 236 (1996).
[8] Y. De Wilde *et al.,* Phys. Rev. Lett. **78**, 4273 (1997).
[9] M. R. Eskildsen *et al.,* Phys. Rev. Lett. **78**, 1968 (1997).
[10] V. G. Kogan *et al.,* Phys. Rev. B **55**, 8693 (1997).
[11] A. E. Koshelev and I. Aranson (to be published).
[12] P. C. Hohenberg and N. R. Werthamer, Phys. Rev. **153**, 493 (1967).
[13] L. P. Gorkov, Soviet Phys. JETP **10**, 593 (1960); **10**, 998 (1960).
[14] L. F. Mattheis, Phys. Rev. B **49**, 13 279 (1994).
[15] J. Yull Rhee, X. Wang, and B. N. Harmon, Phys. Rev. B **51**, 15 585 (1995); the Fermi surface averages used here are $\langle v^2\rangle = 5.12\ 10^{14}$, $\langle v_x^2\rangle = 1.87\ 10^{14}$, $\langle v_z^2\rangle = 1.38\ 10^{14}$, $\langle v_x^4\rangle = 1.44\ 10^{29}$, $\langle v_x^2 v_y^2\rangle = 1.85\ 10^{28}$, $\langle v_x^2 v_z^2\rangle = 1.97\ 10^{28}$, $\langle v_z^4\rangle = 5.85\ 10^{28}$, (in cm^2/sec^2 and cm^4/sec^4, respectively).
[16] M. Xu *et al.,* Physica (Amsterdam) **235C–240C**, 2533 (1994).
[17] S. Kalavathi *et al.,* Physica (Amsterdam) **223B&224B**, 96 (1996); K. Ghosh *et al.,* Physica (Amsterdam) **223B&224B**, 109 (1996).
[18] H. Takagi *et al.,* Physica (Amsterdam) **228C**, 389 (1994).
[19] E. Johnston-Halperin *et al.,* Phys. Rev. B **51**, 12 852 (1995).
[20] For a review, see "Anisotropy Effects in Superconductors," edited by H. Weber (Plenum Press, New York, 1977).
[21] D. K. Christen *et al.,* Physica (Amsterdam) **135B**, 369 (1985); E. J. Kramer and G. S. Knapp, J. Appl. Phys. **46**, 4595 (1975).
[22] M. R. Skokan, R. C. Morris, and W. G. Moulton, Phys. Rev. B **13**, 1077 (1976).
[23] E. Helfand and N. R. Werthamer, Phys. Rev. B **147**, 288 (1966); H. Teichler, in Ref. [20], p. 7; K. Takanaka, in Ref. [20], p. 93.
[24] K. Takanaka, Phys. Status Solidi (b) **68**, 623 (1975); H. Teichler *ibid.* **72**, 211 (1975).
[25] K. Takanaka and K. Kuboya, Phys. Rev. Lett. **75**, 323 (1995).
[26] W. K. Kwok (unpublished).